Supplement of Atmos. Chem. Phys., 26, 8753–8764, 2026
https://doi.org/10.5194/acp-26-8753-2026-supplement


Atmospheric Chemistry and Physics
Open Access

*Supplement of*

# Critical role of dust induced electrostatic coagulation in the evolution of aerosol size distributions in the atmosphere

**Luoqiu Quan et al.**

*Correspondence to:* Xiaohui Lu (luxiaohui@fudan.edu.cn) and Xiaofei Wang (xiaofeiwang@fudan.edu.cn)

**This file includes 13 Figures and 5 Tables:**

**Supplementary Figure S1.** Schematic drawing of the experimental setup for dust aerosol measurement.

**Supplementary Figure S2.** Experimental setup for measuring the charged fraction of dust aerosols.

**Supplementary Figure S3.** Charged fractions of the eight dust aerosol samples.

**Supplementary Figure S4.** Experimental setup for measuring the electrical mobility diameter of ambient aerosols.

**Supplementary Figure S5.** Electrical mobility data for the eight dust aerosol samples.

**Supplementary Figure S6.** Evolution of the particle charge distribution during electrostatic coagulation in a dust-only aerosol system at 25 ℃ with an initial number concentration of 50 #/cm$^3$.

**Supplementary Figure S7.** Evolution of the particle charge distribution during electrostatic coagulation in a dust-only aerosol system at 25 ℃ with an initial number concentration of 100 #/cm$^3$.

**Supplementary Figure S8.** Evolution of the particle charge distribution during electrostatic coagulation in a dust-only aerosol system at 25 ℃ with an initial number concentration of 200 #/cm$^3$.

**Supplementary Figure S9.** Evolution of the particle charge distribution during electrostatic coagulation in a dust-only aerosol system at 25 ℃ with an initial number concentration of 300 #/cm$^3$.

**Supplementary Figure S10.** Evolution of the particle charge distribution during electrostatic coagulation in a dust-only aerosol system at 25 ℃ with an initial number concentration of 500 #/cm$^3$.

**Supplementary Figure S11.** Evolution of the particle charge distribution during electrostatic coagulation in a dust-only aerosol system at 25 ℃ with an initial number concentration of 1000 #/cm$^3$.

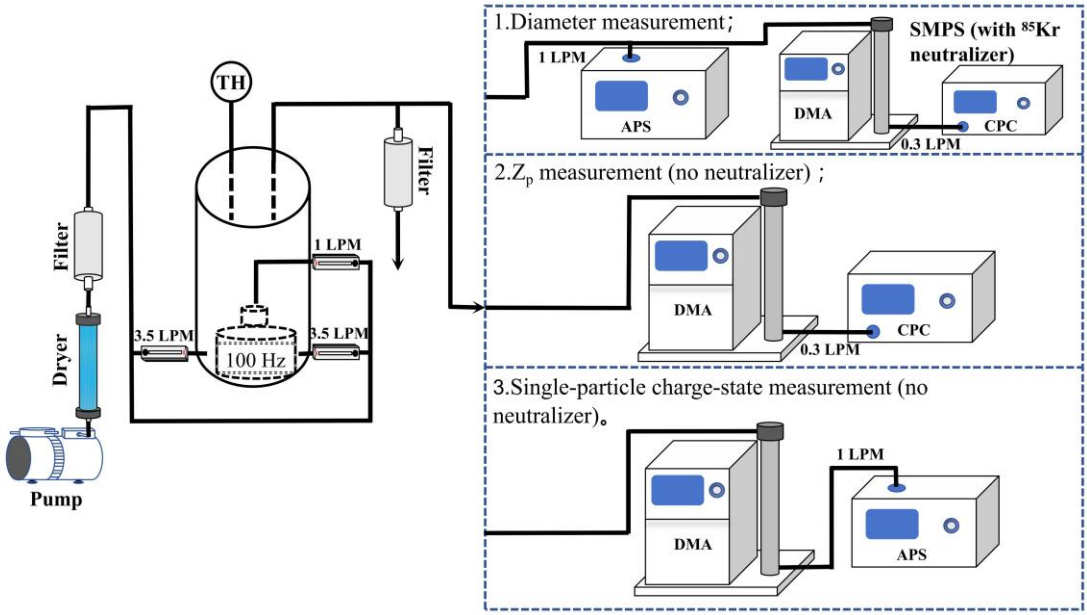


**Figure S1.** Schematic drawing of the experimental setup for dust aerosol measurement.

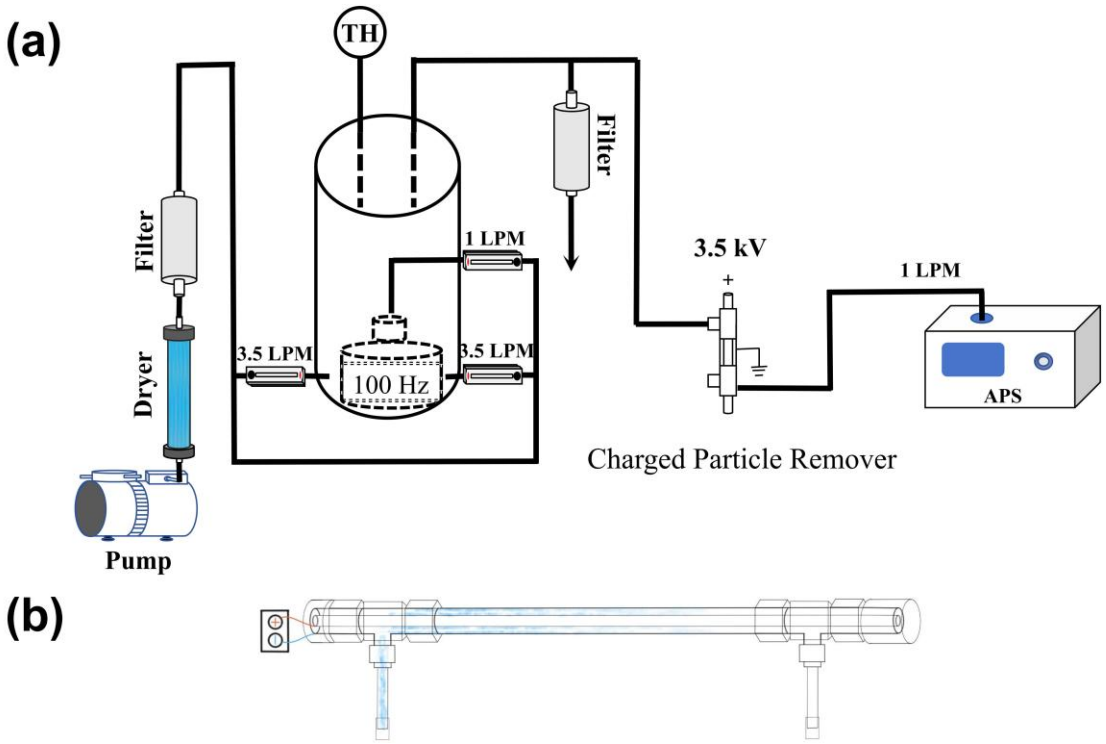


**Figure S2.** Experimental setup for measuring the charged fraction of dust aerosols. (a) Schematic of the setup used to measure the charged fraction of dust aerosols. (b) Geometry and operating parameters of the Charged Particle Remover (CPR), which consists of two coaxially aligned stainless-steel tubes: the inner tube has an outer diameter of 6.35 mm and the outer tube has an inner diameter of 14 mm; the length from inlet to outlet is 50 mm. The inner and outer tubes are connected to the positive and negative terminals of an adjustable high-voltage power supply, respectively.

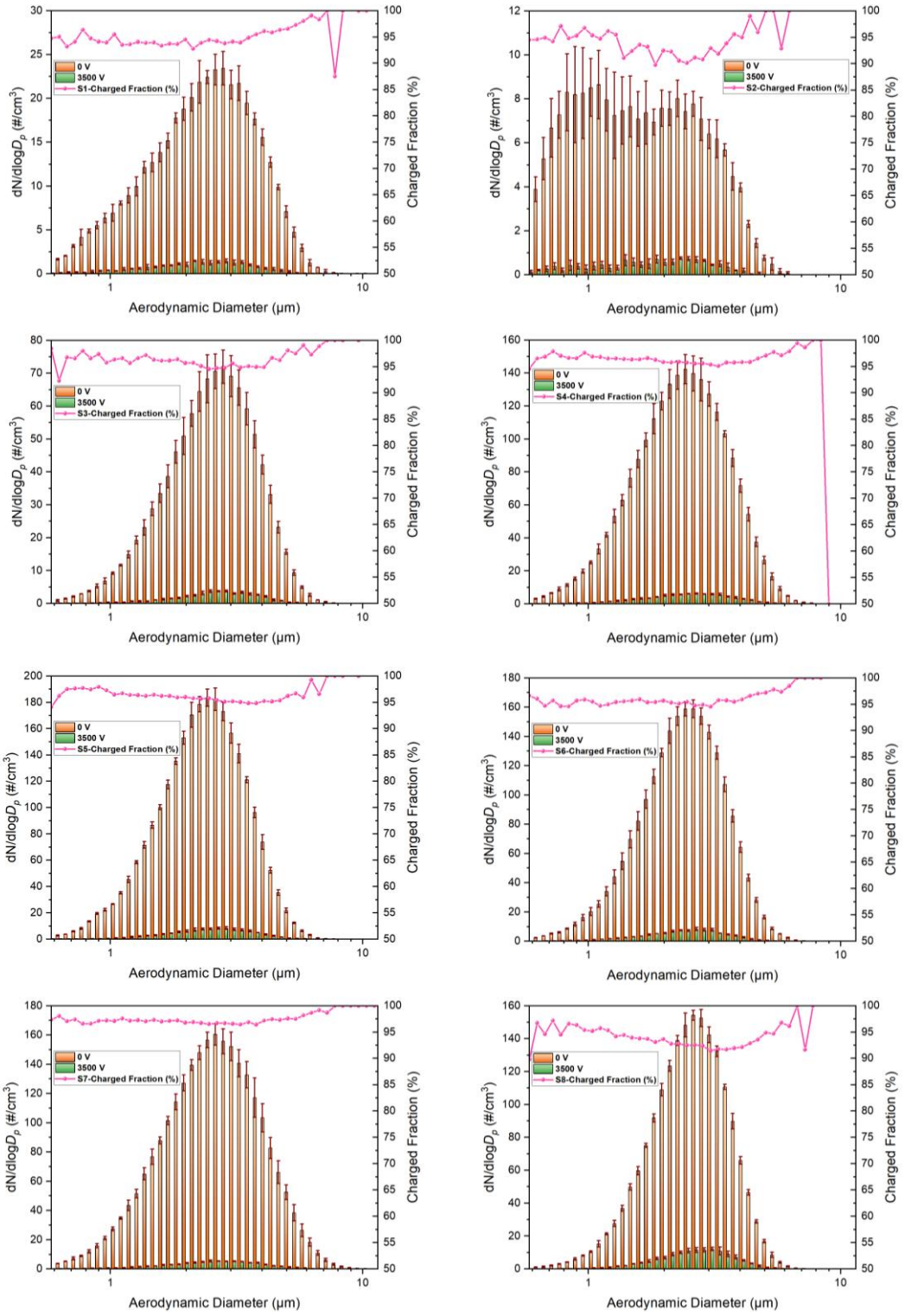


**Figure S3.** Charged fractions of the eight dust aerosol samples. Green and orange bars show the PSDs measured under 0 V and 3500 V, respectively. The pink line denotes the charged fraction as a function of aerodynamic diameter (0.5–10 μm). Sample IDs are indicated in the legend.

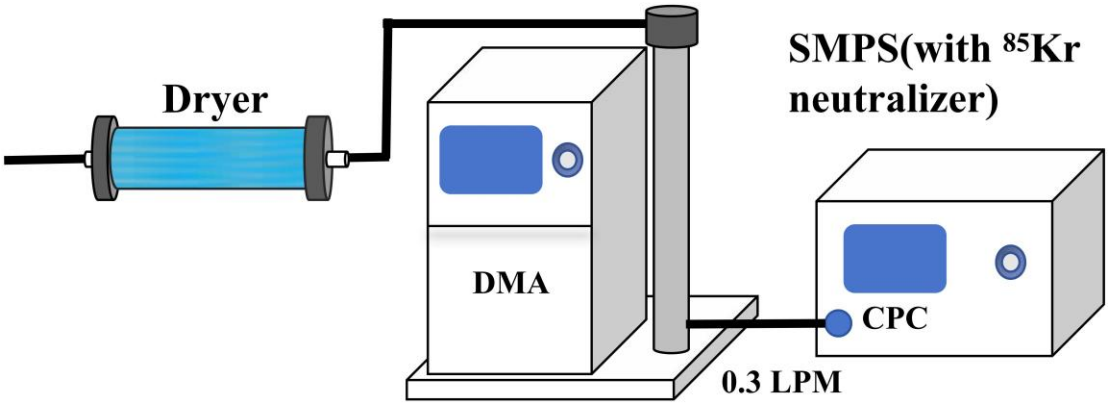


**Figure S4.** Experimental setup for measuring the electrical mobility diameter of ambient aerosols.

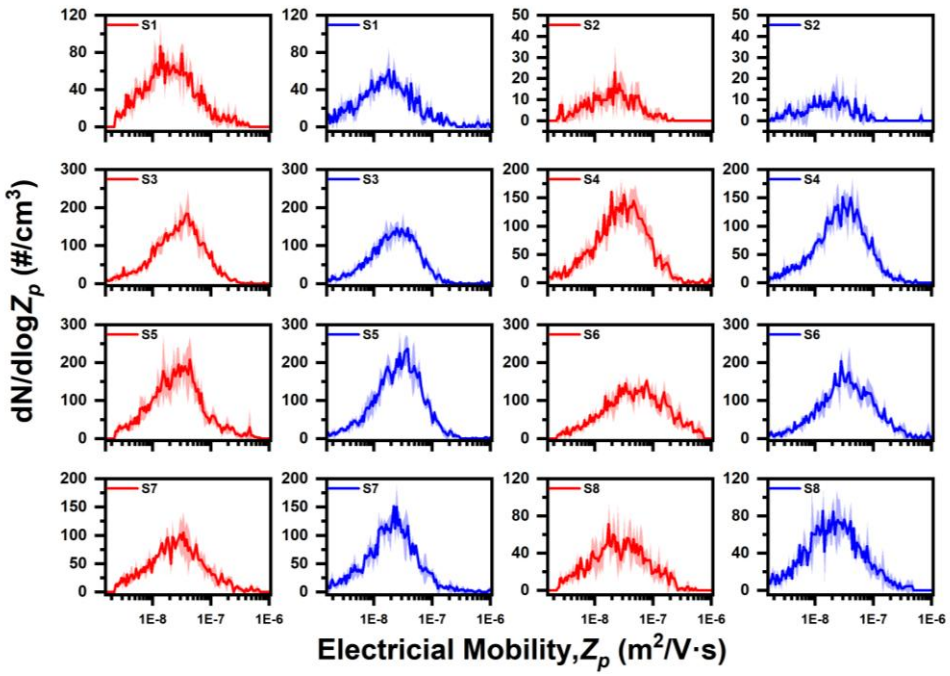


**Figure S5.** Electrical mobility data for the eight dust aerosol samples. Red indicates positively charged particles, and blue indicates negatively charged particles.

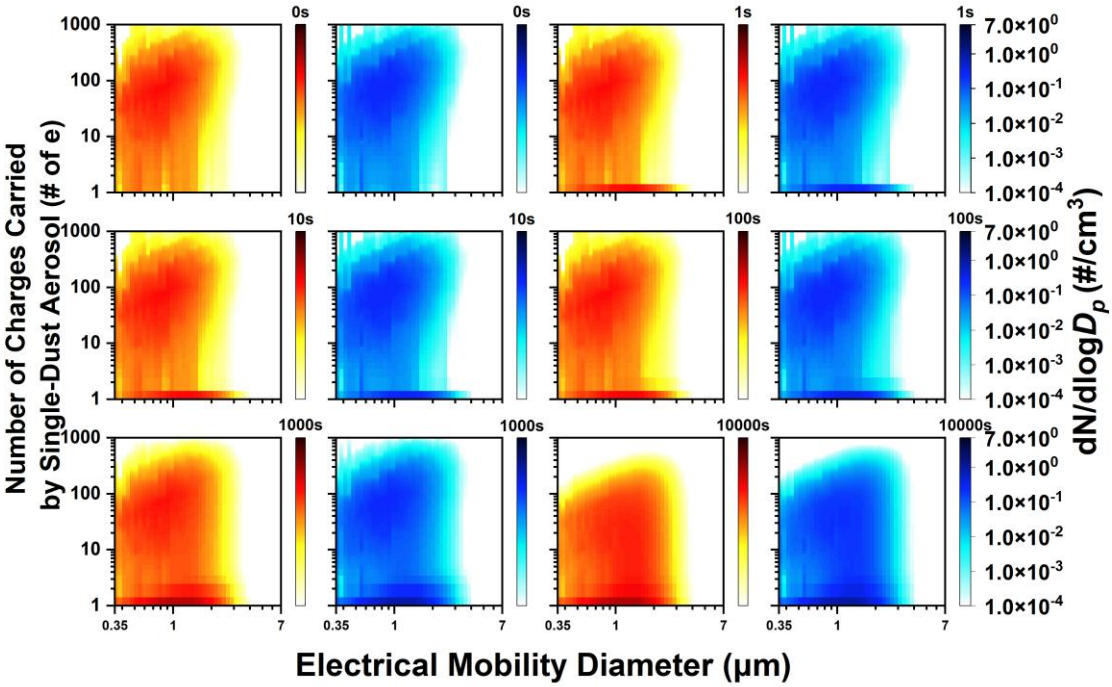


**Figure S6.** Evolution of the particle charge distribution during electrostatic coagulation in a dust-only aerosol system at 25 ℃ with an initial number concentration of 50 #/cm$^3$.

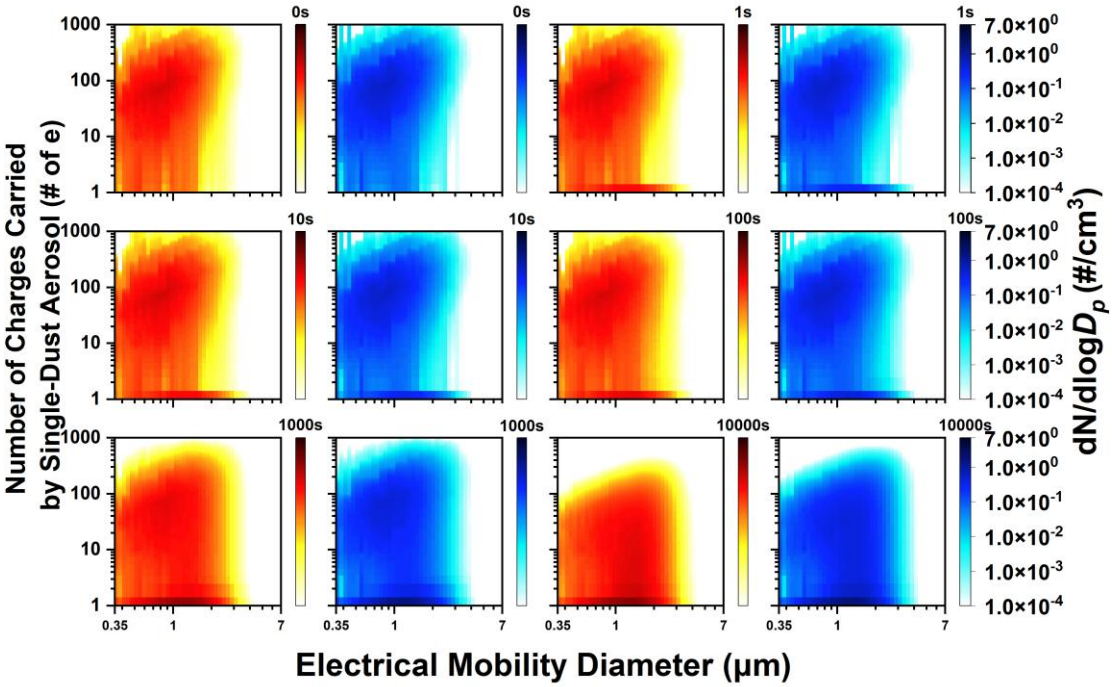


**Figure S7.** Evolution of the particle charge distribution during electrostatic coagulation in a dust-only aerosol system at 25 ℃ with an initial number concentration of 100 #/cm$^3$.

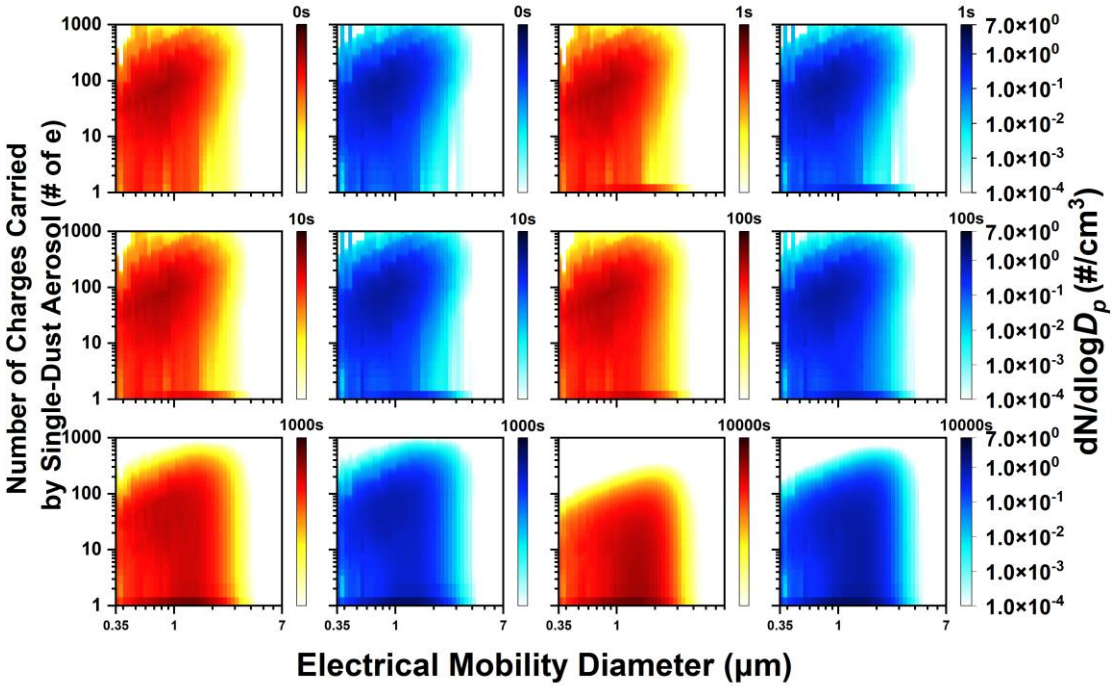


**Figure S8.** Evolution of the particle charge distribution during electrostatic coagulation in a dust-only aerosol system at 25 ℃ with an initial number concentration of 200 #/cm$^3$.

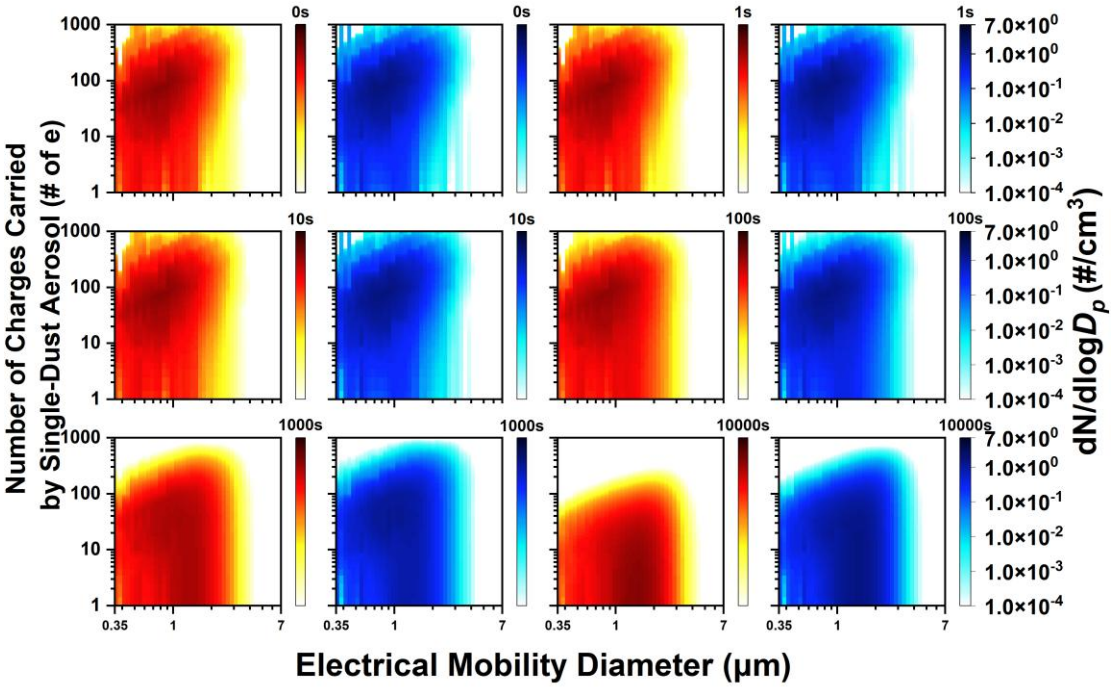


92

93 **Figure S9.** Evolution of the particle charge distribution during electrostatic coagulation
94 in a dust-only aerosol system at 25 ℃ with an initial number concentration of 300 #/cm$^3$.

95

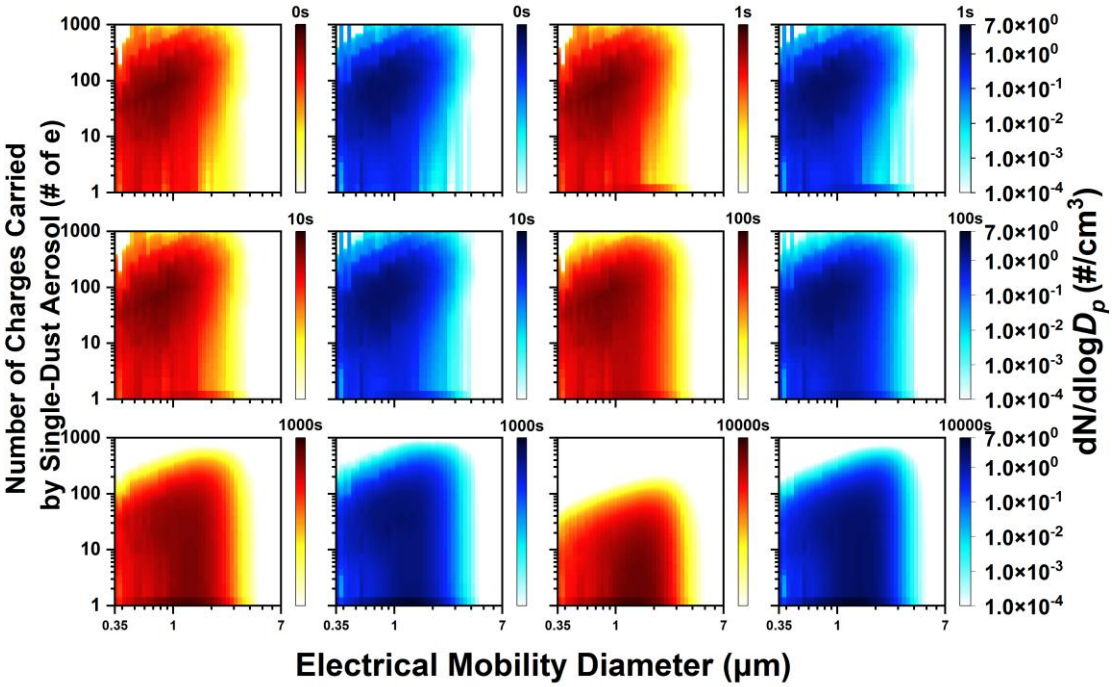


96

97 **Figure S10.** Evolution of the particle charge distribution during electrostatic coagulation
98 in a dust-only aerosol system at 25 ℃ with an initial number concentration of 500 #/cm$^3$.

99

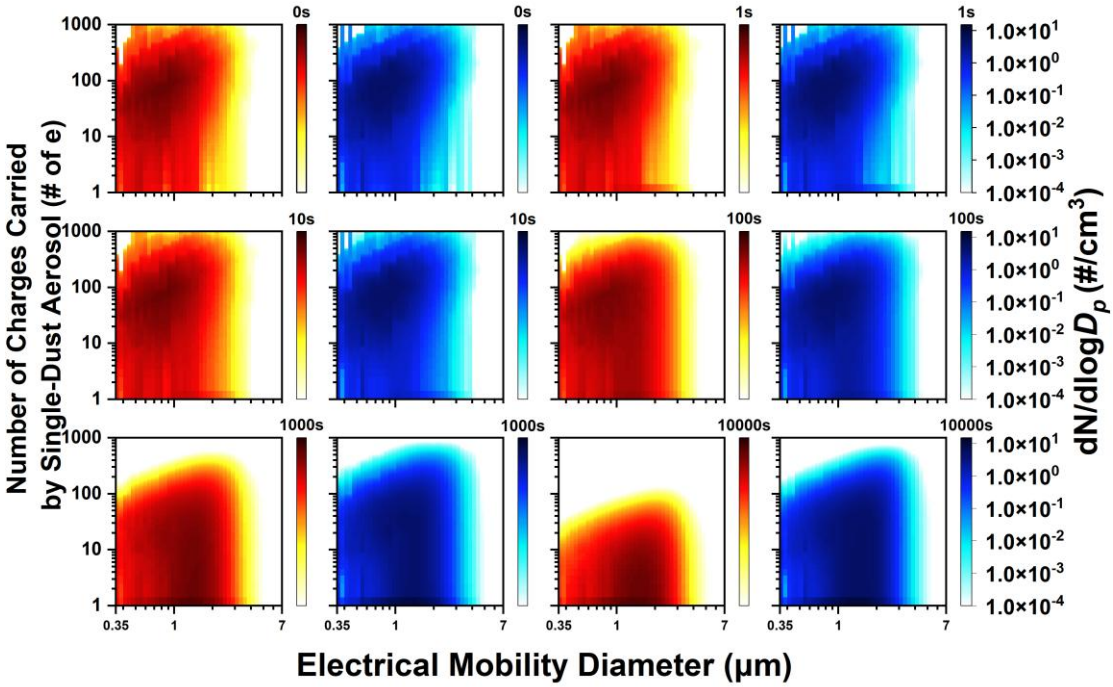


100

101 **Figure S11.** Evolution of the particle charge distribution during electrostatic coagulation
102 in a dust-only aerosol system at 25 °C with an initial number concentration of 1000 #/cm$^3$.
103 The color bar indicates number concentration (dN/dlog$D_p$, #/cm$^3$) and is capped at 15
104 #/cm$^3$.

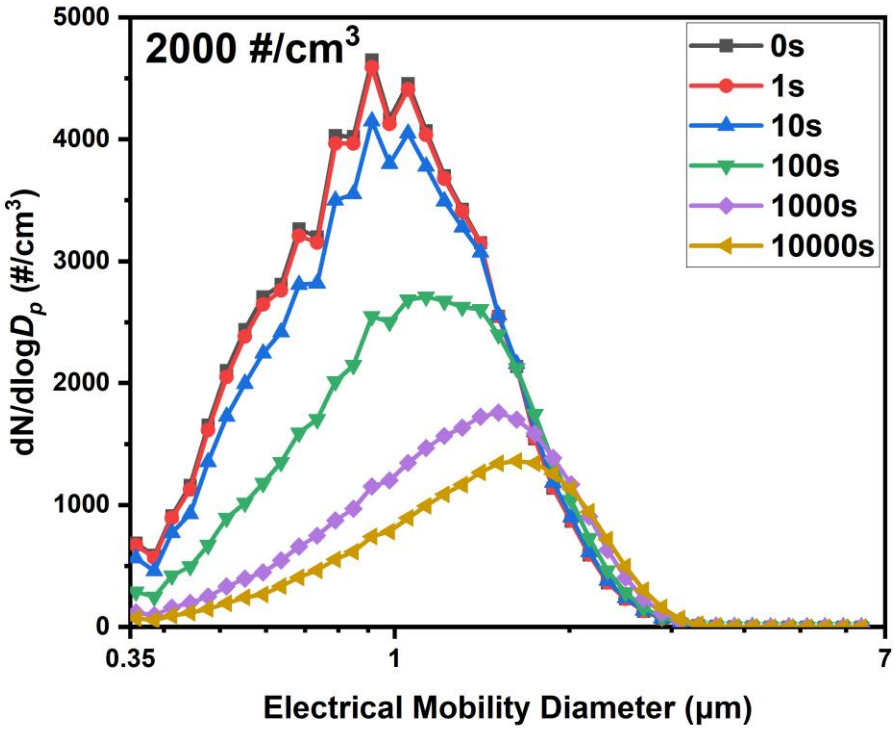


105

106 **Figure S12.** Evolution of the PSD during electrostatic coagulation in a dust-only aerosol
107 system at 25 ℃ with an initial number concentration of 2000 #/cm$^3$.

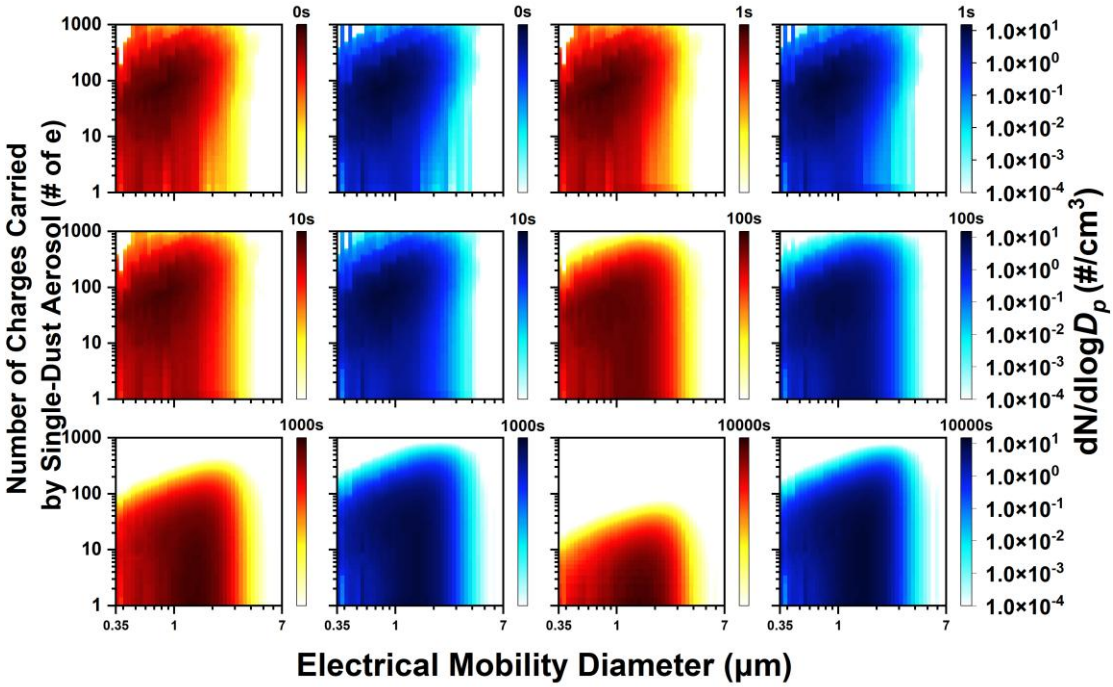


**Figure S13.** Evolution of the particle charge distribution during electrostatic coagulation in a dust-only aerosol system at 25 °C with an initial number concentration of 2000 #/cm$^3$. The color bar indicates number concentration (dN/dlog$D_p$, #/cm$^3$) and is capped at 15 #/cm$^3$.

**Table S1.** Soil sampling locations and soil textures.

| Soils | Location | Soil Texture |
|---|---|---|
| S1 | E 93.8641° N 40.3535° | sand |
| S2 | E 94.6694° N 40.0875° | sand |
| S3 | E 113.2347° N 41.0082° | loamy sand |
| S4 | E 113.2245° N 41.0020° | silt loam |
| S5 | E 111.7782° N 40.9207° | silt loam |
| S6 | E 120.9210° N 31.0780° | silt loam |
| S7 | E 121.5277° N 31.3361° | loam |
| S8 | E 105.2029º N 30.4996º | silty clay loam |

**Table S2.** DMA operating electrical mobility $Z_p$ set points for selecting dust aerosols with specific electrical mobilities.

| No. | $Z_p$ ($m^2 \cdot V^{-1} \cdot s^{-1}$) | Correspondent aerosol diameter at $Z_p$ for a single charge (1e) (μm) | Charge number below which 5% of particles fall | Correspondent diameter at 5% charge (μm) | Median charge number | Correspondent diameter at median charge (μm) | Charge number below which 95% of particles fall | Correspondent diameter at 95% charge (μm) |
|---|---|---|---|---|---|---|---|---|
| 1 | $4.68 \times 10^{-9}$ | 0.197 | 4 | 0.784 | 9 | 1.765 | 32 | 6.275 |
| 2 | $7.83 \times 10^{-9}$ | 0.118 | 5 | 0.586 | 16 | 1.875 | 56 | 6.563 |
| 3 | $1.36 \times 10^{-8}$ | 0.068 | 11 | 0.742 | 26 | 1.754 | 101 | 6.815 |
| 4 | $2.48 \times 10^{-8}$ | 0.037 | 19 | 0.703 | 50 | 1.85 | 178 | 6.586 |
| 5 | $4.64 \times 10^{-8}$ | 0.02 | 37 | 0.732 | 91 | 1.8 | 334 | 6.605 |
| 6 | $8.95 \times 10^{-8}$ | 0.01 | 70 | 0.718 | 186 | 1.907 | 657 | 6.736 |
| 7 | $1.76 \times 10^{-7}$ | 0.005 | 135 | 0.704 | 340 | 1.773 | 874 | 4.557 |
| 8 | $3.51 \times 10^{-7}$ | 0.003 | 299 | 0.782 | 567 | 1.482 | 932 | 2.437 |
| 9 | $7.03 \times 10^{-7}$ | 0.001 | 563 | 0.735 | 725 | 0.946 | 957 | 1.249 |

**Table S3.** Ambient particles locations. The sampling inlet was located on the seventh floor, approximately 20 m above ground level.

| Fine Particulate Matter | Location |
|---|---|
| FuDan University | E 121.5210° N 31.3260° |

**Table S4.** Boltzmann equilibrium charge-state probabilities (z = −6 to +6 e).

| | | Fraction of Total Particle Concentration That Carries This Number (-6 to +6) of Charges | | | | | | | | | | | | |
|---|---|---|---|---|---|---|---|---|---|---|---|---|---|---|
| particle Diameter Midpoint, (nm) | Mobility Midpoint $m^2/v{\cdot}s$ | -6 | -5 | -4 | -3 | -2 | -1 | 0 | +1 | +2 | +3 | +4 | +5 | +6 |
| 14.33 | 1.03E-02 | 0 | 0 | 0 | 0 | 0 | 0.07740 | 0.86198 | 0.06060 | 0 | 0 | 0 | 0 | 0 |
| 16.55 | 7.77E-03 | 0 | 0 | 0 | 0 | 0 | 0.09030 | 0.83938 | 0.07030 | 0 | 0 | 0 | 0 | 0 |
| 19.11 | 5.86E-03 | 0 | 0 | 0 | 0 | 0 | 0.10470 | 0.81425 | 0.08100 | 0 | 0 | 0 | 0 | 0 |
| 22.07 | 4.43E-03 | 0 | 0 | 0 | 0 | 0.00040 | 0.12050 | 0.78618 | 0.09280 | 0.00020 | 0 | 0 | 0 | 0 |
| 25.48 | 3.35E-03 | 0 | 0 | 0 | 0 | 0.00080 | 0.13750 | 0.75588 | 0.10540 | 0.00040 | 0 | 0 | 0 | 0 |
| 29.43 | 2.54E-03 | 0 | 0 | 0 | 0 | 0.00150 | 0.15540 | 0.72334 | 0.11880 | 0.00090 | 0 | 0 | 0 | 0 |
| 33.98 | 1.93E-03 | 0 | 0 | 0 | 0 | 0.00290 | 0.17390 | 0.68883 | 0.13270 | 0.00170 | 0 | 0 | 0 | 0 |
| 39.24 | 1.47E-03 | 0 | 0 | 0 | 0 | 0.00510 | 0.19260 | 0.65272 | 0.14670 | 0.00290 | 0 | 0 | 0 | 0 |
| 45.32 | 1.12E-03 | 0 | 0 | 0 | 0 | 0.00840 | 0.21090 | 0.61545 | 0.16050 | 0.00480 | 0 | 0 | 0 | 0 |
| 52.33 | 8.53E-04 | 0 | 0 | 0 | 0 | 0.01310 | 0.22820 | 0.57755 | 0.17370 | 0.00750 | 0 | 0 | 0 | 0 |
| 60.43 | 6.54E-04 | 0 | 0 | 0 | 0 | 0.01950 | 0.24400 | 0.53969 | 0.18570 | 0.01110 | 0 | 0 | 0 | 0 |
| 69.78 | 5.03E-04 | 0 | 0 | 0 | 0 | 0.02780 | 0.25760 | 0.50260 | 0.19630 | 0.01570 | 0 | 0 | 0 | 0 |
| 80.58 | 3.89E-04 | 0 | 0 | 0 | 0.00120 | 0.03790 | 0.26860 | 0.46539 | 0.20500 | 0.02130 | 0.00050 | 0 | 0 | 0 |
| 93.06 | 3.01E-04 | 0 | 0 | 0 | 0.00260 | 0.04970 | 0.27660 | 0.43040 | 0.21150 | 0.02800 | 0.00120 | 0 | 0 | 0 |
| 107.46 | 2.35E-04 | 0 | 0 | 0.00010 | 0.00510 | 0.06280 | 0.28120 | 0.39728 | 0.21550 | 0.03560 | 0.00230 | 0 | 0 | 0 |
| 124.09 | 1.84E-04 | 0 | 0 | 0.00040 | 0.00910 | 0.07670 | 0.28250 | 0.36632 | 0.21690 | 0.04390 | 0.00410 | 0.00010 | 0 | 0 |
| 143.3 | 1.45E-04 | 0 | 0 | 0.00100 | 0.01460 | 0.09090 | 0.28040 | 0.33774 | 0.21580 | 0.05250 | 0.00660 | 0.00040 | 0 | 0 |
| 165.48 | 1.15E-04 | 0 | 0.00010 | 0.00230 | 0.02200 | 0.10470 | 0.27510 | 0.31172 | 0.21220 | 0.06120 | 0.00990 | 0.00080 | 0 | 0 |
| 191.1 | 9.23E-05 | 0 | 0.00030 | 0.00440 | 0.03090 | 0.11740 | 0.26710 | 0.28841 | 0.20650 | 0.06940 | 0.01390 | 0.00150 | 0.00010 | 0 |
| 220.67 | 7.43E-05 | 0.00010 | 0.00090 | 0.00770 | 0.04110 | 0.12850 | 0.25680 | 0.26786 | 0.19890 | 0.07680 | 0.01850 | 0.00260 | 0.00020 | 0 |
| 254.83 | 6.02E-05 | 0.00020 | 0.00190 | 0.01250 | 0.05220 | 0.13760 | 0.24480 | 0.25006 | 0.18980 | 0.08290 | 0.02340 | 0.00430 | 0.00050 | 0 |
| 294.27 | 4.91E-05 | 0.00050 | 0.00370 | 0.01870 | 0.06340 | 0.14430 | 0.23160 | 0.23483 | 0.17970 | 0.08730 | 0.02840 | 0.00640 | 0.00100 | 0.00010 |
| 339.82 | 4.04E-05 | 0.00120 | 0.00660 | 0.02620 | 0.07420 | 0.14860 | 0.21780 | 0.22184 | 0.16900 | 0.09010 | 0.03330 | 0.00900 | 0.00170 | 0.00020 |
| 392.42 | 3.34E-05 | 0.00250 | 0.01080 | 0.03480 | 0.08420 | 0.15050 | 0.20390 | 0.21058 | 0.15810 | 0.09100 | 0.03780 | 0.01200 | 0.00280 | 0.00050 |
| 453.16 | 2.77E-05 | 0.00460 | 0.01620 | 0.04400 | 0.09290 | 0.15030 | 0.19040 | 0.20035 | 0.14740 | 0.09030 | 0.04170 | 0.01510 | 0.00430 | 0.00090 |
| 523.3 | 2.32E-05 | 0.00790 | 0.02290 | 0.05340 | 0.10010 | 0.14810 | 0.17770 | 0.19035 | 0.13720 | 0.08830 | 0.04490 | 0.01830 | 0.00600 | 0.00160 |
| 604.3 | 1.94E-05 | 0.01230 | 0.03050 | 0.06230 | 0.10560 | 0.14450 | 0.16610 | 0.17970 | 0.12780 | 0.08540 | 0.04740 | 0.02140 | 0.00800 | 0.00250 |
| 697.83 | 1.63E-05 | 0.01800 | 0.03860 | 0.07050 | 0.10930 | 0.13980 | 0.15600 | 0.16748 | 0.11940 | 0.08210 | 0.04900 | 0.02420 | 0.01020 | 0.00360 |
| 805.84 | 1.38E-05 | 0.02460 | 0.04690 | 0.07750 | 0.11130 | 0.13450 | 0.14750 | 0.15282 | 0.11210 | 0.07890 | 0.04990 | 0.02660 | 0.01230 | 0.00500 |

The equation is as follows:

$$f(N)=10^{\left[\sum_{i=0}^{5} a_i(N)\left(\log\frac{D_p}{\mathrm{nm}}\right)^i\right]} \quad (1)$$

Applicable aerosols size range:

$$1\ \mathrm{nm} \le D_p \le 1000\ \mathrm{nm} \text{ for } N = -1, 0, 1$$

$$20\ \mathrm{nm} \le D_p \le 1000\ \mathrm{nm} \text{ for } N = -2, 2$$

| $a_i(N)$ | $N$=-2 | $N$=-1 | $N$=0 | $N$=1 | $N$=2 |
|---|---|---|---|---|---|
| $a_0$ | -26.3328 | -2.3197 | -0.0003 | -2.3484 | -44.4756 |
| $a_1$ | 35.9044 | 0.6175 | -0.1014 | 0.6044 | 79.3772 |
| $a_2$ | -21.4608 | 0.6201 | 0.3073 | 0.4800 | -62.8900 |
| $a_3$ | 7.0867 | -0.1105 | -0.3372 | 0.0013 | 26.4492 |
| $a_4$ | -1.3088 | -0.1260 | 0.1023 | -0.1553 | -5.7480 |
| $a_5$ | 0.1051 | 0.0297 | -0.0105 | 0.0320 | 0.5049 |

For the fraction of particles carrying three or more charges, use Equation which is based on a derivation by Gunn from 1956:

$$f(N) = \frac{e}{\sqrt{4\pi^2 \varepsilon_0 D_p kT}} \exp \frac{-[N - \frac{2\pi\varepsilon_0 D_p kT}{e^2} \ln(\frac{Z_{i+}}{Z_{i-}})]^2}{2\frac{2\pi\varepsilon_0 D_p kT}{e^2}} \quad (2)$$

Where $e$ ($1.60217733 \times 10^{-19}$ C) is elementary charge, $\varepsilon_0$ ($8.854187817 \times 10^{-12}$ F/m) is dielectric constant, $D_p$ (m) is electrical mobility diameter, $T$ (K) is Temperature, $N$ is number of elementary charge units, $\frac{Z_{i+}}{Z_{i-}}$ (0.875,Wiedensohler, A. 1988) is ion mobility ratio.

**Table S5.** Size-bin edges (sorted in ascending order by column)

| Background (non-dust) ambient aerosol size-bin edges (14.1–346 nm; 90 edges) | | | | | | | | |
|---|---|---|---|---|---|---|---|---|
| 14.1 | | 31.1 | | 68.5 | | 151.2 | | 333.8 |
| 14.6 | | 32.2 | | 71 | | 156.8 | | 346 |
| 15.1 | | 33.4 | | 73.7 | | 162.5 | | |
| 15.7 | | 34.6 | | 76.4 | | 168.5 | | |
| 16.3 | | 35.9 | | 79.1 | | 174.7 | | |
| 16.8 | | 37.2 | | 82 | | 181.1 | | |
| 17.5 | | 38.5 | | 85.1 | | 187.7 | | |
| 18.1 | | 40 | | 88.2 | | 194.6 | | |
| 18.8 | | 41.4 | | 91.4 | | 201.7 | | |
| 19.5 | | 42.9 | | 94.7 | | 209.1 | | |
| 20.2 | | 44.5 | | 98.2 | | 216.7 | | |
| 20.9 | | 46.1 | | 101.8 | | 224.7 | | |
| 21.7 | | 47.8 | | 105.5 | | 232.9 | | |
| 22.5 | | 49.6 | | 109.4 | | 241.4 | | |
| 23.3 | | 51.4 | | 113.4 | | 250.3 | | |
| 24.1 | | 53.3 | | 117.6 | | 259.5 | | |
| 25 | | 55.2 | | 121.9 | | 269 | | |
| 25.9 | | 57.3 | | 126.3 | | 278.8 | | |
| 26.9 | | 59.4 | | 131 | | 289 | | |
| 27.9 | | 61.5 | | 135.8 | | 299.6 | | |
| 28.9 | | 63.8 | | 140.7 | | 310.6 | | |
| 30 | | 66.1 | | 145.9 | | 322 | | |

| Dust aerosol size-bin edges (0.358–6.37 μm; 41 edges). | | | | | | | | |
|---|---|---|---|---|---|---|---|---|
| 0.358 | | 0.684 | | 1.308 | | 2.499 | | 4.776 |
| 0.385 | | 0.735 | | 1.406 | | 2.685 | | 5.132 |
| 0.413 | | 0.79 | | 1.51 | | 2.886 | | 5.515 |
| 0.444 | | 0.849 | | 1.623 | | 3.101 | | 5.926 |
| 0.477 | | 0.913 | | 1.744 | | 3.333 | | 6.37 |
| 0.513 | | 0.98 | | 1.874 | | 3.581 | | |
| 0.552 | | 1.054 | | 2.014 | | 3.848 | | |
| 0.593 | | 1.132 | | 2.164 | | 4.135 | | |
| 0.637 | | 1.217 | | 2.326 | | 4.444 | | |

142